High Spatial Resolution Gamma Imaging Detector Based on a 5" Diameter R3292 Hamamatsu PSPMT

R. Wojcik[1], S. Majewski[1], B. Kross[1], D. Steinbach[2], A.G. Weisenberger [1]
[1]Jefferson Lab., 12000 Jefferson Ave., Newport News, VA 23606
[2]College of William and Mary Physics Dept., Williamsburg, VA 23187

Abstract

High resolution imaging gamma-ray detectors were developed using Hamamatsu's 5" diameter R3292 position sensitive PMT (PSPMT) [1] and a variety of crystal scintillator arrays. Special readout techniques were used to maximize the active imaging area while reducing the number of readout channels. Spatial resolutions approaching 1 mm were obtained in a broad energy range from 20 to 511 keV. Results are also presented of coupling the scintillator arrays to the PMT via imaging light guides consisting of acrylic optical fibers.

I. INTRODUCTION

The need for high resolution gamma cameras in many fields continues to grow. In nuclear medicine current commercial systems using multiple PMTs and a slab of scintillator can only resolve cancers on the order of a cm whereas, in the new fields of scintimammography and positron emission mammography, doctors need to see cancers as small as a few mm. In the case of studying gene expression in small animals a resolution of about 1 mm is needed [2]. One commercial solid state imaging system using Cadmium Zinc Telluride [3] is trying to fill the need for higher resolutions, however, the stopping power is limited to energies less than 200 keV and the price is significantly higher than a PMT-crystal system. Several recent efforts have described the use of small gamma cameras based on PSPMTs [4-10]. Our goal is to develop a cost effective high resolution imaging system for a broad energy range (20 to 511 keV).

II. EXPERIMENTAL SETUP

A. PMT and Electronics

Hamamatsu's R3292 has a proximity focused parallel dynode mesh structure with crossed wire anodes. The x and y coordinates consist of 28 wires apiece and the active area of the PMT is 11 cm in diameter. To reduce the number of individual analogue readout channels while still retaining the advantages of a local readout (as opposed to integral readout methods such as current division or delay lines), we grouped the anode wires into sectors with two to four wires per sector (fig. 1). The advantages of local readout include high rate operation, less edge distortion, and the ability to apply a special truncated center of gravity (COG) technique, mentioned below, to maximize the active imaging area. Each anode sector was amplified before being sent over a coaxial ribbon cable to the data acquisition system. The data acquisition system was based on LeCroy's FERA ADC's and a Macintosh Power PC running Kmax data acquisition software [11]. The last dynode was used to trigger the discriminator and provide a gate to the ADCs.

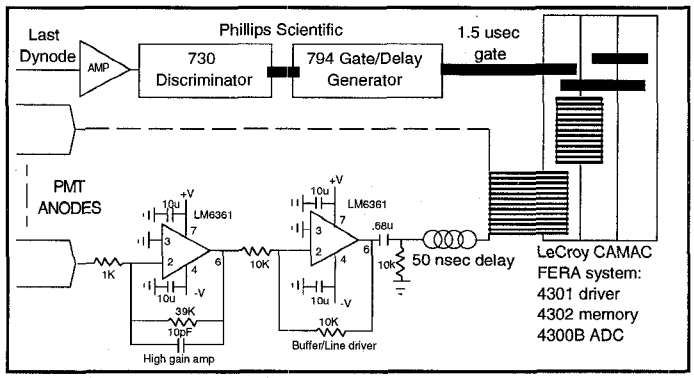

Figure 1: PMT readout electronics.

B. Crystal arrays and Energies

Through previous work we found that, from a selection of the most popular crystal scintillators (YAP, CsI(Na), BGO, NaI(Tl), GSO, and LSO), only CsI(Na), NaI(Tl), and GSO are prime candidates for nuclear medicine gamma cameras [12]. YAP and BGO are ruled out due to relatively low light output and LSO is naturally radioactive and, at this time, not readily commercially available. All of the arrays are made up of small square scintillator pixels arranged in an approximately 11 cm diameter circle. We also tested a NaI(Tl) slab for comparison. Crystal arrays are preferable over slabs of scintillators because of the spatial non-uniformities found in most PSPMTs (fig. 2). There is, however, a small loss in energy resolution. By being able to identify the particular pixel light came from, image distortion correction is easily implemented. The size of the pixel is important in optimizing the trade-off between spatial resolution and having enough light delivered to the PMT for crystal identification and energy determination. The thickness of the array was selected to optimize the tradeoff between stopping power and efficient light transfer to the PMT, again effecting energy resolution. In general, energy resolution is important for rejecting scattered radiation which blurs the image.

All of the arrays except for the GSO array were manufactured by various companies [13-16] by taking a slab of the material and sectioning it with a fine diamond saw. The crystals are separated by approximately .25 mm with the region between the crystals filled with an opaque white reflective material. The GSO array is hand assembled from pixels which only have their output face polished. The other 5 sides are left rough cut and no optical separation is used. The NaI(Tl) arrays and slab are enclosed in .5 mm thick Al with a 1 mm quartz window.

U.S. Government Work Not Protected by U.S. Copyright

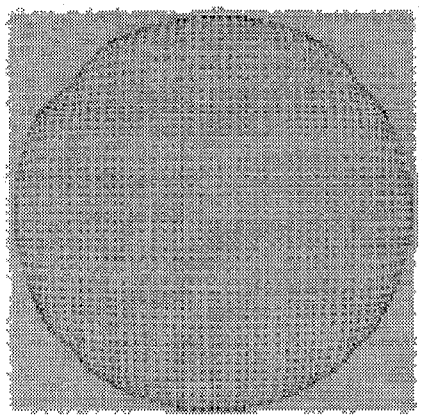

Figure 2: Image of a uniformly ^{57}Co irradiated 11 cm diameter array of 2x2x6 mm^3 CsI(Na) pixels. Spatial non-uniformities caused by the PSPMT structure are clearly seen.

Depending on the energy range of interest, different crystal arrays were tested. For lower energies (22 keV to 140 keV), comparisons were made between CsI(Na) and NaI(Tl) arrays. For higher energies (511 keV annihilation gammas), the GSO array was used. Table 1 shows the relevant parameters of each crystal array while table 2 shows the radioactive sources and the main energy component used in these tests. The lower energy sources (22-35 keV) are used in small animal gene research while the middle energy (122 keV) is very close to that used in scintimammography (^{99m}Tc at 140 keV). The highest energy sources are used to simulate positron emission tomography.

Table 1
Scintillator arrays used in tests.

Array type	Pixel size (mm^2)	Thickness (mm)	Light output (Rel. to NaI)	Density (g/cc)
NaI(Tl) slab	N/A	6	100%	3.67
NaI(Tl)	2x2	6		
NaI(Tl)	3x3	10		
CsI(Na)	2x2	3	65-83%	4.51
CsI(Na)	2x2	6		
CsI(Na)	1x1	3		
GSO(Ce)	3x3	10	20-25%	6.71

Table 2
Radioactive sources used in tests.

Radioactive source	Relevant energy (keV)
^{109}Cd	22
^{125}I	27-35
^{57}Co	122
^{99m}Tc	140
^{22}Na	511
^{137}Cs	624

C. *Software calculations and Image Reconstruction*

Once the signals have been converted by the ADC and had their pedestals subtracted, a truncated COG calculation is performed to obtain the x and y coordinates of the event. The methodology of the truncation is that the values of all the signals on one axis are summed together and only those signals above a predefined fraction (f-factor) of the sum are used to calculate the COG. This approach compensates for the physical truncation caused by the edge of the PMT (fig. 3). By an optimized implementation of this technique we have been able to greatly increase the active imaging area of the PMT.

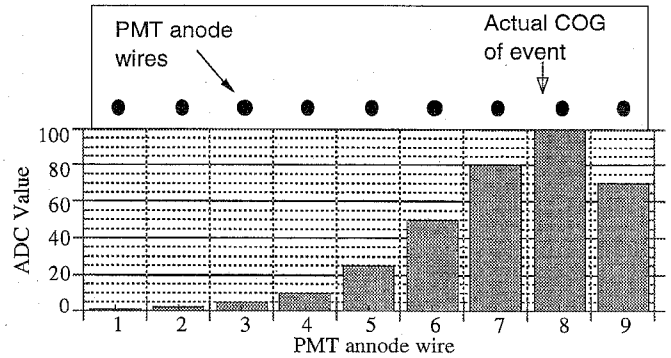

Figure 3. Performing a COG calculation using all the Measured ADC data gives a value of 7.2 for the position of the event while using only those values above 10% (f-factor = 0.1) of the sum gives a value of 7.6; much closer to the actual location.

During a flood source calibration run where the whole crystal is irradiated by a radioactive point source placed ~10 cm above the array, each crystal pixel appears as a well defined and separated spot on the image. One then identifies a region belonging to each pixel so that any x-y coordinate can thus be associated with a particular crystal pixel. Once this is completed, the energy spectrum for each pixel is measured and used to set an energy acceptance window on the ADC data from each pixel. This adjusts for any gain variations across the face of the PMT while also rejecting the lower energy events which have been scattered within the object before reaching the scintillator and thus do not correspond to the primary radiation one is trying to image. The final image is obtained by remapping the electronically measured coordinates of the crystals to the physical locations and smoothing the image.

III. Results

A. *Truncated COG*

The result of the truncated COG algorithm is readily apparent in figure 4. Using a Pb mask of 1 mm diameter holes spaced 1 cm apart on the NaI(Tl) slab we obtained an image using ^{99m}Tc. The image on the left was acquired using the standard COG routine while the one on the right was acquired using the truncated COG routine with an f-factor of 0.1. Using the standard COG the last two holes at the edges overlap and can not be distinguished.

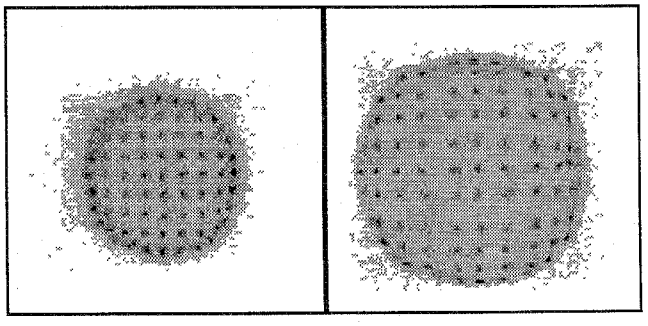

Figure 4: Application of truncated COG on NaI(Tl) slab with lead mask irradiated with ^{99m}Tc. Both images are in the same scale.

B. *Optical coupling and Energy Resolution*

In general, we found one should not use optical coupling grease with scintillator arrays due to the enhanced acceptance of wide angle photons (fig. 5). With optical coupling grease the wide angle photons from a crystal pixel which would have been totally internally reflected are now transferred to the PMT causing a large increase in the measured pixel spot size. With air coupling, most of the angled photons are at least partially reflected at the interface thus greatly narrowing the acceptance angle at the photocathode producing a well defined pixel spot. This is dramatically illustrated in figure 6 where the 2x2x3 mm^3 crystals of CsI(Na) in the image became totally indistinguishable when grease was used.

Using the NaI(Tl) slab to test the effect of optical coupling on the energy resolution we found only a minor improvement (going from 14.2% without optical coupling to 12.5% with coupling at 140 keV) even though the amplitude of the signal increased by a factor of 1.7 (fig. 7). There was a noticeable degradation to the energy resolution by going to a pixel array, however, it is still quite easy to reject scattered gammas. There is only a minor difference in the energy resolution between the NaI(Tl) (22.8%) and CsI(Na) (23.8%) arrays (fig. 8).

C. *GSO crystal array*

Unfortunately, GSO can not be grown in large sizes and thus the inexpensive technique of slicing up a slab of the material is not possible. Thus, in order to keep costs down, we tested manufacturing an array by using individual pixels which only had one face polished. The remaining faces were left rough cut. Our hand assembly job did not produce the most uniform array, however, all the 3x3x10 mm^3 pixels are clearly separated even though the crystals were not optical isolated (fig. 9). The energy resolution at 511 keV was found to be 19.2%.

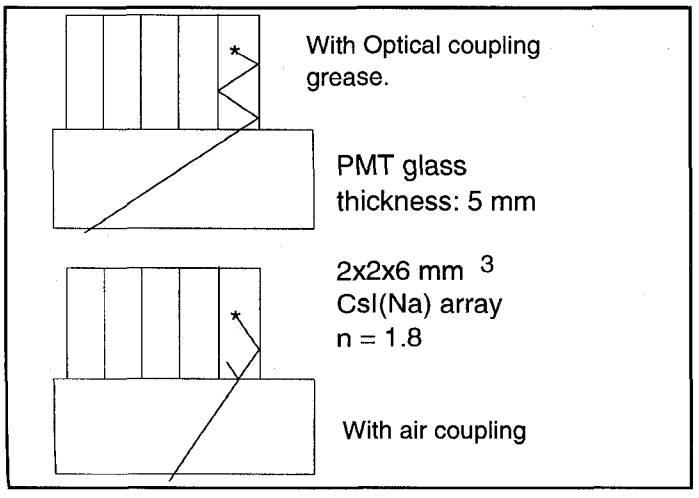

Figure 5: With optical coupling grease wide angle photons cause a blurring of the image while with air coupling these photons are rejected by total internal reflection.

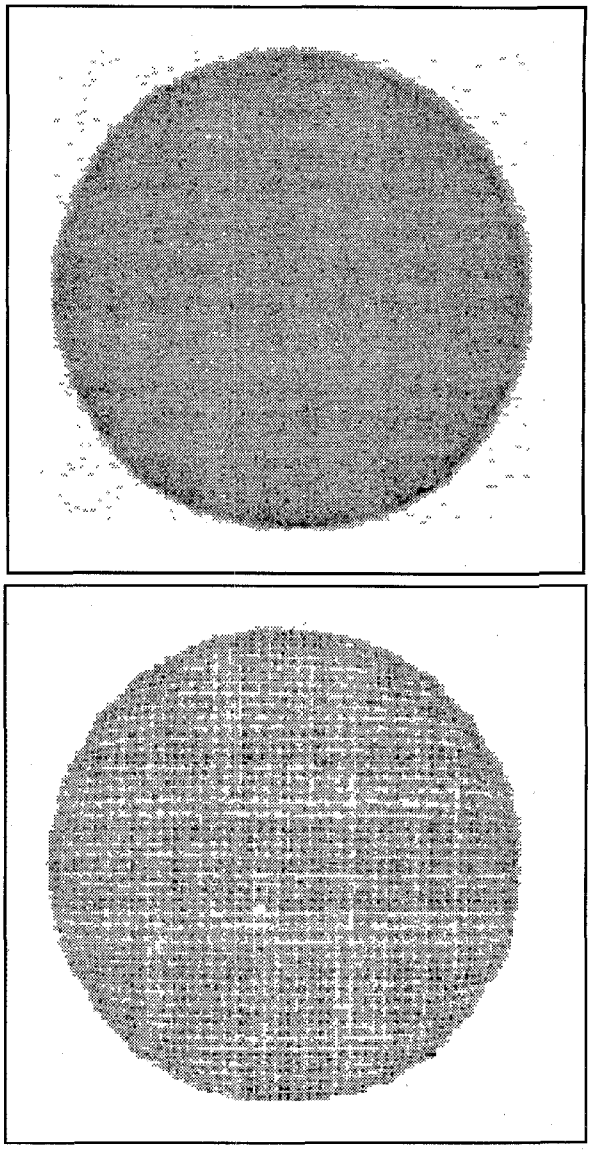

Figure 6: The effect of using optical coupling grease (top) vs. no grease (bottom) on the 2x2x3 mm^3 array of CsI(Na) irradiated with 140 keV ^{99m}Tc.

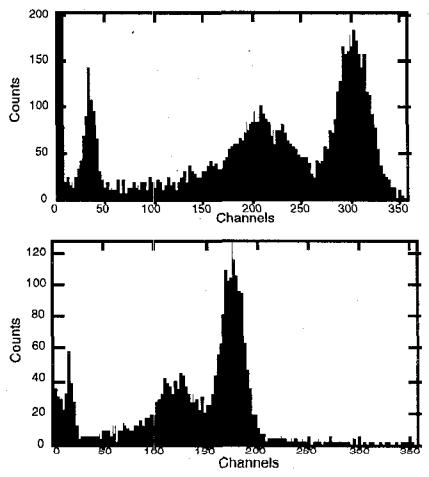

Figure 7: Effect of optical coupling grease (top) vs. no grease (bottom) on light output and energy resolution with the NaI(Tl) slab irradiated by 140 keV ^{99m}Tc.

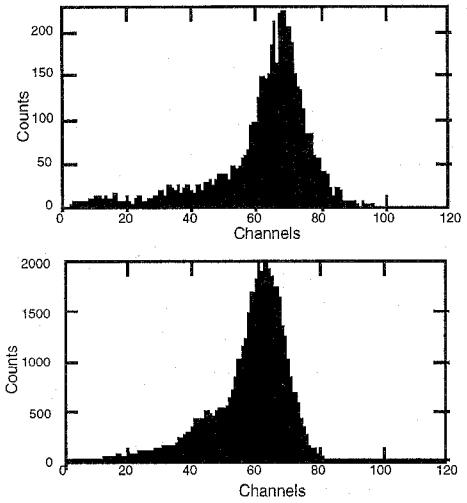

Figure 8: There are only minor differences in the energy resolution between the 2x2x6 mm^3 array of NaI(Tl) (top) and the 2x2x3 mm^3 array of CsI(Na) (bottom) irradiated by 140 keV ^{99m}Tc.

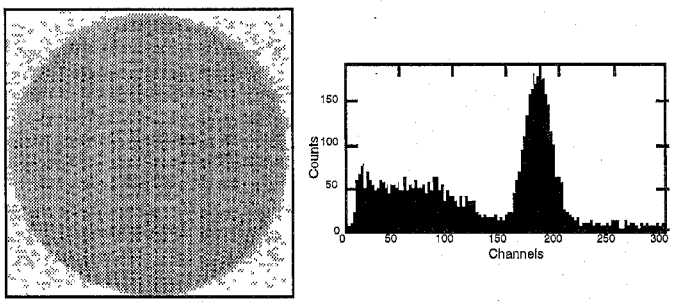

Figure 9: Image of 3x3x10 mm^3 GSO array irradiated by 511 keV ^{22}Na (left) and the energy spectrum from the four central pixels (right).

D. *Very High Resolution Gamma Camera*

For small animal gene research, needing the highest spatial resolutions, a CsI(Na) array with 1x1x3mm^3 pixels was tested. We were unable to resolve the individual crystal elements using ^{125}I. However, they were clearly seen when we used ^{137}Cs (figs. 10, 11). This allows us to map out the spatial and gain variations of the crystals using the higher energy source and apply these corrections to imaging ^{125}I. Preliminary results using phantoms have been quite promising and live animal studies will begin in the near future [17].

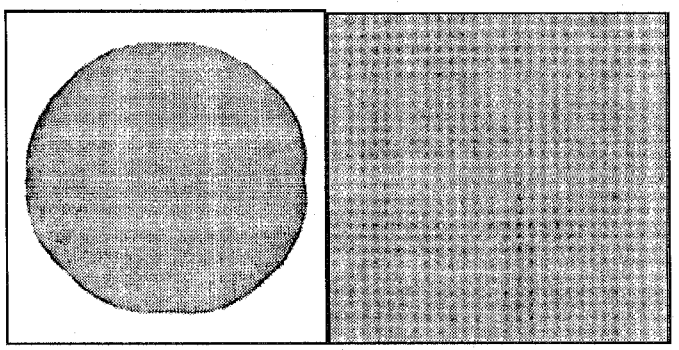

Figure 10: Image of the full 1x1x3 mm^3 CsI(Na) array irradiated by 624 keV ^{137}Cs (left). Enlargement of a 3x3 cm^2 area (right).

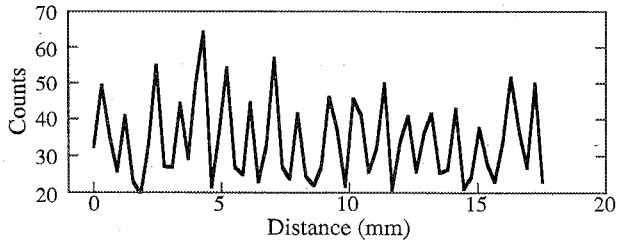

Figure 11: Projection across one of the rows of the CsI(Na) array in figure 10.

IV. Light Guide Coupling

An 11.5 cm diameter imaging light guide was constructed by gluing together 15 cm long 3 mm diameter acrylic-clad polystyrene fibers. The NaI(Tl) array of 3x3x10 mm^3 pixels was then coupled to the light guide using optical grease [18]. It can be seen that separation of individual crystals at 122 keV is very good (fig. 12). Unfortunately the energy resolution was rather poor (85% at 122 keV), however, we plan to implement double-clad 2 mm diameter fibers to improve both the spatial and energy resolution. Such light guide couplers can be used whenever available space does not allow for a PMT to be placed next to the scintillator or when there is a need to eliminate the dead region around the perimeter of the sensor head. They can also be used to build high resolution large area detectors with no dead area by adapting a square scintillator array to the round PMT and butting these units together.

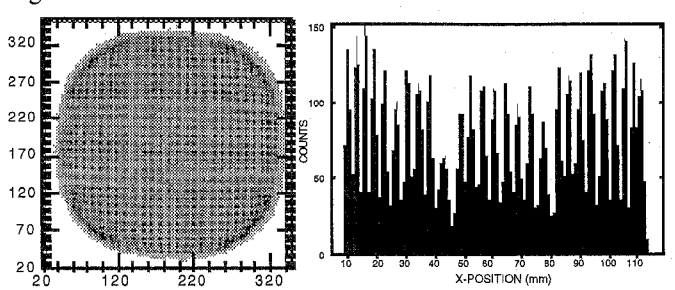

Figure 12: NaI(Tl) array coupled to PSPMT via imaging light guide irradiated with ^{57}Co. Raw 2D image is shown at left with a projection of one of the columns shown in the histogram.

V. Conclusions

It seen that the 5" diameter R3292 PSPMT can form the basis for a high spatial resolution gamma imager with an 11 cm diameter active field of view. A spatial resolution approaching 1 mm can be obtained in a broad energy range from 20 to 511 keV when properly sized arrays of bright crystal scintillators are used. The crystal array of choice for lower energy applications is CsI(Na). Since CsI(Na) is only slightly hydroscopic it is not required to be enclosed. Thus CsI(Na) does not have the added window between the crystals and PMT to worsen the resolution like NaI(Tl). For higher energies, GSO is currently the best choice due to its stopping power and availability. For an economical and high spatial resolution readout, one should employ readout sections made of 2-4 anode wires with a truncated center of gravity algorithm. Potential applications of such a detector include small animal imaging, scintimammography, and positron emission mammography, as well as gamma imaging in astrophysics and other fields.

VI. ACKNOWLEDGMENTS

The authors would like to thank Dr. Mark Williams from the University of Virginia (UVa) for the many useful discussions and his permission to perform some of the measurements at UVa. Allen Goode and Burl Manis of UVa are also thanked for their assistance.

VII. REFERENCES

[1] Hamamatsu Photonics, 360 Foothill Road, Bridgewater, NJ 08807.

[2] A.G. Weisenberger, E. Bradley, S. Majewski and M. Saha, "Development of a Novel Radiation Imaging Detector System for *In Vivo* Gene Imaging in Small Animal Studies", *Conference Record of the 1996 IEEE Medical Imaging Conference*, pp. 1201-1205, 1996.

[3] Digirad Corporation, 7408 Trade Street, San Diego, CA 92121-2410.

[4] Jens Michael Poulsen, Roberto Verbeni and Filippo Frontera, "Position-sensitive scintillation detector for hard X-rays" *Nuclear Instruments and Methods in Physics Research* A310 (1991) pp. 398-402.

[5] T.D.Milster, J.N. Aarsvold, H.H. Barrett, A.L.Landesman, L.S.Mar, D.D.Patton, T.J.Roney, R.K.Rowe, and R.H.Seacat III, "A Full-Field Modular Gamma Camera" *J Nucl Med* 1990; 31: pp. 632-639.

[6] NJ Yasillo, RA Mintzer, JN Aarsvold, KL Matthews, SJ Heimsath, CE Ordonez, X Pan, Cwu, TA Block, RN Beck, C-T Chen, And M Cooper: "A Single-Tube Miniature Gamma Camera" IEEE pp. 1073-1076.

[7] C.E.Ordonez, R.A.Mintzer, JN.Aarsvold, N.J.Yasillo, and K.L Matthews: "Simulation of Imaging with Sodium Iodide Crystals and Position-Sensitive Photomultiplier Tubes" *IEEE Transactions on Nuclear Science*, Vo. 41, No 4, August 1994, pp. 1510-1515.

[8] Z.He, A.J.Bird, D.Ramsden: "A 5 Inch Diameter Position-Sensitive Scintillation Counter" *IEEE Transations on Nuclear Sience*, Vol. 40, No.4, Aug. 1993 pp. 447-451.

[9] L.H.Barone, K.Blazek, D.Bollini, A.Del Guerra, F. de Notaristefani, G.De Vincenis, G.Di Domenico, M. Galli, M. Giganti, P.Maly, R.Pani, R. Pellegrini, A.Pergola, A.Piffanilli, F.Scopinaro, A.Soluri, F. Vittori: "Toward a Nuclear Medicine with Sub-Millimeter Spatial Resolution." *Nuclear Instruments and Methods in Physics Research* A 360 (1995) pp. 302-306.

[10] R.Pani, F.Scopinaro, G.Depola, R.Pellegrini, A.Soluri; "Very High Resolution Gamma Camera Based on Position Sensitive Photomultiplier Tube." *Physica Medica* - Vol. IX, N. 2-3, April-September 1993.

[11] Sparrow Corporation, PO Box 6102, Mississippi State, MS 39762.

[12] D. Steinbach et al., "A Small Scintimammography Detector Based on a 5" PSPMT and Crystal Scintillator Arrays", these proceedings .

[13] The NaI(Tl) arrays were manufactured by Scionix, Holland B.V., CC Bunnik, The Netherlands.

[14] The CsI(Na) arrays were manufactured by Hilger Analytical Crystal Materials Group, Westgood, Margate Kent CT9-4JL, United Kingdom

[15] The NaI(Tl) slab was acquired from Isotope Products, 1811 North Keystone St., Burbank, CA 91504.

[16] The GSO pixels were acquired from Marubeni Specialty Chemical Inc., 10 Bank Street, Suite 740, White Plains, NY 10606.

[17] Visc-60M siloxane grease manufactured by General Electric Company, Waterford, NY 12188.

[18] AG Weisenberger et al., "Design Features and Performance of a CsI(Na) Array Based Gamma Camera for Small Animal Gene Research", these proceedings .